Higher-Order Harmonic Generation from Fullerene by Means of the Plasma Harmonic Method

R. A. Ganeev,[1,2] L. B. Elouga Bom,[1] J. Abdul-Hadi,[1] M. C. H. Wong,[3] J. P. Brichta,[3] V. R. Bhardwaj,[3] and T. Ozaki[1]

[1]*Institut National de la Recherche Scientifique, Énergie, Matériaux et Télécommunications, 1650 Lionel-Boulet, Varennes, Québec J3X 1S2, Canada*

[2]*Scientific Association Akadempribor, Academy of Sciences of Uzbekistan, Akademgorodok, Tashkent 100125, Uzbekistan*

[3]*Department of Physics, University of Ottawa, 150 Louis Pasteur, Ottawa, Ontario K1N 6N5, Canada*

(Received 29 August 2008; published 5 January 2009)

We demonstrate, for the first time, high-order harmonic generation from C_{60} by an intense femtosecond Ti:sapphire laser. Laser-produced plasmas from C_{60}-rich epoxy and C_{60} films were used as the nonlinear media. Harmonics up to the 19th order were observed. The harmonic yield from fullerene-rich plasma is about 25 times larger compared with those produced from a bulk carbon target. Structural studies of plasma debris confirm the presence and integrity of fullerenes within the plasma plume, indicating fullerenes as the source of high-order harmonics.

DOI: 10.1103/PhysRevLett.102.013903 PACS numbers: 42.65.Ky, 52.38.Mf, 78.67.Bf

High-order harmonic generation (HHG) is a well-demonstrated method for producing coherent extreme ultraviolet (XUV) radiation. HHG in atoms or molecules is a three-step process [1] where (i) the incident laser field removes the electron from its ground state to the continuum, (ii) the electron wave packet propagates in the laser field and returns to the parent ion, and (iii) the electron wave packet recombines emitting high-energy photons. The resultant harmonic spectrum exhibits a rapid decrease in harmonic intensity for the lower orders, followed by plateaulike distribution of higher-order harmonics, and finally a cutoff. HHG opens new frontiers in science by extending nonlinear optics and time-resolved spectroscopy to the XUV region [2] and pushing ultrafast science to the attosecond domain, enabling XUV spectroscopy and imaging of molecular orbital [3], surface dynamics [4], and electron motion. HHG is the only route to produce attosecond light pulses [5,6] and is therefore fundamental to attosecond science [7]. However, such applications require high HHG conversion efficiency, which still remains an obstacle.

Often, rare gas atoms are used as a nonlinear medium to produce high harmonics. The efficiency of the HHG process depends on the density of atoms, phase matching between the harmonic and the fundamental fields, and the absorption of harmonics by the medium. However, use of large molecular systems, clusters, and nanostructured materials can further increase the harmonic yield by exploiting multiple excitation channels and charge delocalization in such systems. Studies on rare gas atomic clusters containing 10^3–10^6 atoms (with cluster sizes of 2–28 nm) demonstrated extended cutoffs and an increase in the harmonic yield due to collective oscillations of electrons [8–10]. Alternatively, one can use nanoparticles as the nonlinear media to produce high harmonics. This approach has been realized recently by using laser-produced plasmas of targets that contain nanoparticles [11].

Molecules provide a unique opportunity to study the HHG process. Systems exhibiting large polarizability (*vis-à-vis* collective motion of electrons) can be potentially used to increase high harmonic yield. Moreover, the HHG process can be influenced by molecular orientation [12,13] and quantum interferences inherent to multielectron systems [14]. The HHG from molecules itself can be used as a versatile tool to probe and characterize the multielectron dynamics and retrieve structural information [3,14,15]. With this aim, HHG in several diatomic, triatomic [14], and organic molecules was studied [16]. As the molecular system increases in complexity, the theory of HHG, which is based on single active electron approximation by assuming that only the valence electron responds to the incident laser field while the other electrons are frozen, has to be modified to include the multielectron dynamics.

In this Letter, we report, to the best of our knowledge, the first experimental observations of high-order harmonics generated in fullerenes produced by laser ablation and compare them with those produced in carbon. In C_{60}, we observe an extended cutoff with harmonics up to the 19th order. The spectrum exhibits an enhancement of the harmonics (11th–15th order) that lie within the plasmon resonance, indicative of the multielectron dynamics. The harmonic yield in fullerenes is 25 times larger compared to carbon.

We choose C_{60} as a nonlinear medium because (i) it is highly polarizable ($\sim$80 Å^3 [17]), (ii) it is stable against fragmentation in intense laser fields due to a very large number of internal degrees of freedom leading to the fast diffusion of the excitation energy, (iii) it exhibits giant plasmon resonance at $\sim$20 eV [18,19], (iv) it has large photoionization cross sections [18,19], and (v) multielectron dynamics is known to influence ionization and recollision [20,21] that are central to HHG process. The saturation intensities of different charge states of C_{60} are higher compared to isolated atoms of similar ionization potential [20,22].

Previous studies on fullerenes have demonstrated generation of second [23], third [24,25], and fifth [26] har-

monics. Experiments on HHG in C_{60} beyond the fifth order do not exist. Theoretical studies on HHG from C_{60} involved extending the three-step model [27] and using dynamical simulations [28]. In the latter, higher-order harmonics were shown to be due to multiple excitations and could be easily generated even with a weak laser field. Both studies reveal how HHG can be used to probe the electronic and molecular structure of C_{60}.

In our studies, we used bulk carbon and two types of fullerene samples as targets for laser ablation. We preferred the laser ablation technique to the conventional ovens to produce a dense jet of C_{60} molecules, which is required for efficient generation of harmonics. In one fullerene sample, the powder (98% $C_{60,}$ 2% $C_{70,}$ Alfa Aestar) was mixed with epoxy and fixed onto glass or silver substrates leading to an inhomogeneous distribution of fullerene nanoparticles. The second sample is a fullerene film on a glass substrate. The films are grown by evaporating C_{60} powder (99 + %, MER Corporation) in a resistively heated oven at 600 °C. The effusive beam of C_{60} molecules is deposited onto a glass substrate maintained at liquid nitrogen temperature. The thickness of the film used in the experiment was about a few microns.

Experiments were carried out at the Canadian Advanced Laser Light Source at the Institut National de la Recherche Scientifique. For laser ablation, a prepulse that was split from the uncompressed Ti:sapphire laser (pulse duration $t = 210$ ps, wavelength $\lambda = 800$ nm, pulse repetition rate 10 Hz) was focused on the target placed in a vacuum chamber by using a plano-convex lens (focal length $f = 150$ mm; see inset in Fig. 1). We adjusted the focal spot diameter of the prepulse beam to be 600 μm on the target surface. The intensity of the subnanosecond prepulse (I_{pp}) on the target surface was varied between 2×10^9 and 2×10^{10} W cm^{-2}. After a delay (variable between 6 and 74 ns), the femtosecond main pulse (pulse energy 8–20 mJ, $t = 35$ fs, $\lambda = 800$ nm) was focused on the plasma from the orthogonal direction using a plano-convex lens (focal length $f = 680$ mm). Our experiments were performed with femtosecond main pulse intensities of up to $I_{fp} = 7 \times 10^{14}$ W cm^{-2}, above which the HHG efficiency considerably decreased due to impeding processes in the laser plasma. The harmonics were spectrally dispersed by an XUV spectrometer with a flat-field grating (1200 lines/mm, Hitachi). The XUV spectrum was then detected by a combination of a microchannel plate and a phosphor screen. The images are recorded using a charge-coupled device camera.

Figure 1 shows the harmonic spectra obtained from ablation of a bulk carbon target, C_{60} powder fixed in epoxy on silver, and C_{60} film. HHG produced in the ablation plume of bulk carbon targets exhibit a plateaulike harmonic spectrum up to the 25th order. To understand the origin of HHG, we studied the structure of the deposited debris. The absence of nanoparticles in the ablation plume

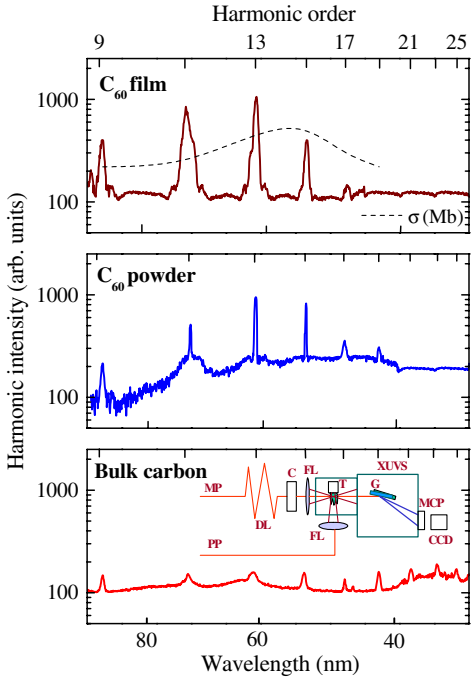

FIG. 1 (color online). Harmonic spectra obtained in the plasma plumes produced from (bottom panel) a bulk carbon target, (middle panel) C_{60} powder-rich epoxy, and (upper panel) C_{60} film. The dashed curve in the top panel corresponds to the photoionization cross sections near plasmon resonance. The inset shows the experimental setup of HHG in fullerenes. MP: main pulse; PP: prepulse; DL: delay line; C: grating compressor; FL: focusing lenses; T: target; XUVS: XUV spectrometer; G: gold-coated grating; MCP: microchannel plate; CCD: charge-coupled device.

of a bulk carbon target suggests carbon monomers as the source of harmonics. We did not observe any specific enhancements in the harmonic yield or extension of cutoff.

The harmonic spectra from targets containing C_{60} powder in epoxy and C_{60} film are significantly different in comparison with the bulk carbon target under identical experimental conditions. (i) Harmonics lying in the spectral range of surface plasmon resonance in C_{60} (20 eV, $\lambda = 62$ nm [8,19]) are enhanced. (ii) The harmonic yields are larger by a factor of 20–25 for the 13th harmonic. (iii) The harmonic cutoff in C_{60} is lower (19th order) than carbon but extends beyond the value (11th order) predicted by the three-step model. (iv) The 11th- and 13th-order harmonics in C_{60} are more intense than the 9th harmonic. Though the sensitivity of our detection system decreases for longer wavelengths at around 70 nm, in most cases, where various bulk targets and atoms were used, we observed a considerably stronger 9th harmonic. The dashed curve in the top panel of Fig. 1 corresponds to the photoionization cross sections near plasmon resonance.

Varying the experimental conditions such as temporal delay between the prepulse and main pulse (6, 24, and 74 ns) and their intensities did not considerably change the

harmonic yield in C_{60}. The delay is not important in C_{60} targets due to lower ablation thresholds. We used a prepulse intensity of 2×10^9 W cm^{-2}, 10 times lower than the bulk carbon target. Increasing the intensity of the femtosecond main pulse did not lead to an extension of the cutoff in fullerenes, which is a sign of saturation of the HHG in this medium. Moreover, at relatively high laser intensities, we observed a decrease in harmonic output. At such intensities, multiple ionization of C_{60} occurs leading to a high free electron density causing phase mismatch. Similarly, an optimal prepulse intensity exists above which harmonics in C_{60} became weaker due to fragmentation of fullerenes, increase of the free electron concentration, phase mismatch, and self-defocusing. By calibrating our detection system using techniques previously reported [29], we estimate the efficiency of the 11th–15th harmonics (between 50–70 nm) from a fullerene plume to be 3×10^{-6}–10^{-5}.

We now address the source of high-order harmonics in fullerene targets. We analyzed the spatial characteristics of the targets prior to laser ablation and compared them with the ablated material debris deposited on nearby substrates (glass, aluminum foil, or silicon wafer) as shown in Fig. 2. Surface morphology of the C_{60} film and the powder in epoxy are shown Figs. 2(a) and 2(c), obtained by an atomic force microscope (AFM). The structure of the C_{60} film is close to the crystalline shape with the mean sizes of crystallites in the range of 80–200 nm. The sample containing C_{60} powder in epoxy suggests C_{60} aggregates whose sizes are in the range of 200–600 nm. In comparison, the size of a single C_{60} molecule is less than 1 nm. Figures 2(b) and 2(d) show the morphology of the debris due to ablation of the C_{60} film and powder imaged by a scanning electron microscope (SEM) and an atomic force microscope, respectively. The ablation debris contains the same aggregated particles as those prior to ablation. We therefore conclude that fullerene clusters are responsible for HHG. Also, no harmonics were observed in our experiments during ablation of pure epoxy and the substrates alone without fullerenes.

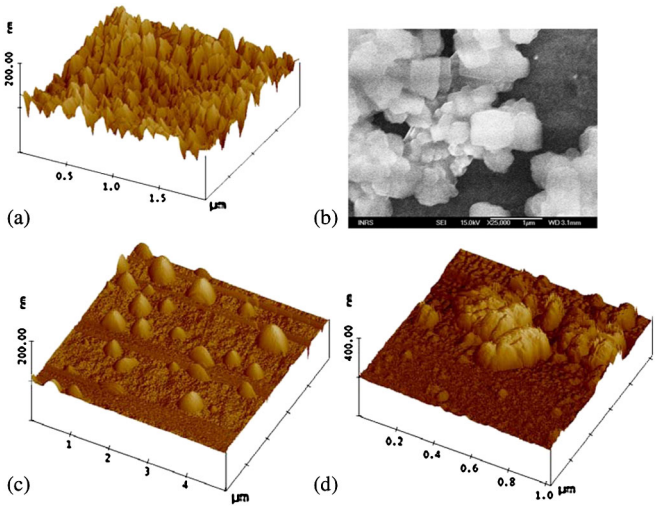

FIG. 2 (color online). (a) AFM image of the fullerene film used for the ablation in the HHG. (b) SEM image of the debris structure after ablation of the C_{60} film and deposition on the Si surface. (c) AFM image of the structure of C_{60} powder. (d) AFM image of the C_{60} powder deposited on the Al substrate during the ablation.

The structural integrity of the fullerenes ablated off the surface should be intact until the driving pulse arrives. So, the prepulse laser intensity is a very sensitive parameter and was kept between 2×10^9 to 8×10^9 W cm^{-2} in our experiments. At lower intensities the concentration of clusters in the ablation plume is low, while at higher intensities one can expect fragmentation. The temperature at the surface after the absorption of a 1 mJ prepulse was estimated to be in the range of 600–700 °C, which was above the evaporation threshold of fullerenes (~300 °C) but below the temperature of fragmentation (~1000 °C). This estimation is valid for both types of fullerene targets.

C_{60} films produced slightly more intense and stable harmonics with low shot-to-shot variation compared to the powder-epoxy mixture. This is due to the homogeneous distribution of particles in the film. In both types of fullerene targets, the density of the ablation plume decreases for successive laser shots due to evaporation of C_{60} from the ablation area. As a result, the harmonic intensity decreases, as shown in Fig. 3 for C_{60} film. After about 10 laser pulses at the same target position, harmonic generation almost disappeared, unless we moved to a fresh spot on the fullerene film. To maintain the stability of the HHG process from C_{60} film, we moved the fullerene film after a few shots, to avoid reduction of fullerene concentration in the ablation plume.

The fullerene density in the interaction region is a critical parameter in efficient generation of high-order harmonics due to a quadratic dependence. However, at high densities, phase mismatch and absorption of harmon-

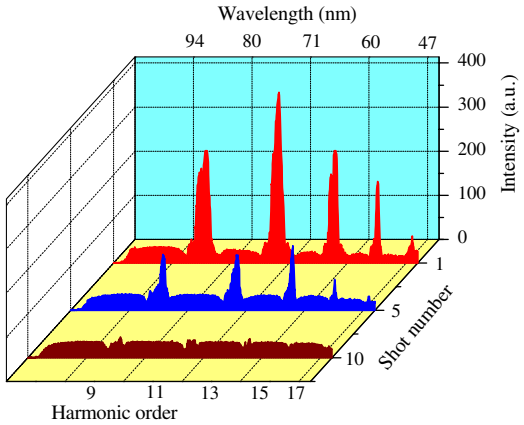

FIG. 3 (color online). Variation of harmonic spectra observed at the consecutive shots on the same spot of fullerene film.

ics begin to dominate and shape the harmonic spectrum. Exact measurement or calculation of fullerene concentration in the ablation plume is difficult. In bulk targets, simulation techniques based on the hydrodynamic code HYADES can accurately predict the atomic concentration [30]. However, when extended to nanoparticle-rich targets they provide only a rough estimate of the density due to a lack of information on the absorbance of these materials. For C_{60} film, we estimate the fullerene density to be no less than 5×10^{16} cm^{-3}. Experimentally, under identical conditions, the thickness of the ablated material from carbon and fullerene targets is found to be the same, suggesting nearly identical densities.

We now discuss the origin of HHG in C_{60}. Specifically, we will focus on two important observations, namely, (1) extension of harmonic cutoff and (2) enhancement of harmonics in the vicinity of plasmon resonance. In the three-step model for HHG, the cutoff harmonic is given by $3.17U_p + I_p$ (where $I_p = 7.6$ eV is the ionization potential of C_{60} and the U_p is the ponderomotive energy). We used an intensity of $\sim 10^{14}$ W cm^{-2} in our measurements, which is above the saturation intensity of the first two charge states of C_{60} [20]. The saturation intensity of C_{60}^{+} is 5×10^{13} W cm^{-2} in close agreement with the theoretical value of 4×10^{13} W cm^{-2} [22]. Accordingly, if the HHG is from neutral C_{60}, the cutoff should be at the 11th harmonic. In contrast, we observe up to the 19th harmonic.

Higher cutoff could be due to (i) the contribution of C_{60} ions to HHG process—laser ablation at prepulse intensities used in the experiment is known to lead to soft ionization identical to matrix-assisted laser desorption or ionization—and (ii) multiphoton excitation of surface plasmon (20 eV) by the incident laser field (1.55 eV). If ionization starts from a plasmon state and the electron returns to the ground state upon recombination, the plasmon energy is converted into photon energy extending the cutoff [31]. (iii) Recombination into orbitals, other than the highest occupied molecular orbital of C_{60}, with higher ionization potentials [32] can result in extension of the cutoff.

In conclusion, we report high-order harmonic generation in fullerenes that exhibit an extended cutoff and enhancement (up to 25 times) of harmonic intensity in the low-energy plateau region compared with those generated from monomer carbon particles. The enhancement is attributed to the multielectron dynamics in C_{60}. Further studies on HHG involving isolated C_{60} molecules irradiated with light pulses at different wavelengths and polarizations would provide deeper insight into the mechanisms responsible for enhancement of high harmonics. Our results along with recent theoretical calculations suggest that (i) multielectron effects will vitiate the process of tomographic imaging of molecular orbitals that involves retrieving the structural information of molecule encoded in the high harmonic spectrum and (ii) systems exhibiting collective oscillations at lower energies, such as small metal clusters, could lead to larger enhancements of high harmonics due to higher probability of exciting multielectron dynamics.

R. A. G. gratefully acknowledges the support from the Natural Sciences and Engineering Research Council of Canada to carry out this work.

[1] P. B. Corkum, Phys. Rev. Lett. **71**, 1994 (1993).
[2] N. A. Papadogiannis *et al.*, Phys. Rev. Lett. **90**, 133902 (2003).
[3] J. Itatani *et al.*, Nature (London) **432**, 867 (2004).
[4] R. I. Tobey *et al.*, Opt. Lett. **32**, 286 (2007).
[5] P. M. Paul *et al.*, Science **292**, 1689 (2001).
[6] M. Drescher *et al.*, Science **291**, 1923 (2001).
[7] P. B. Corkum and F. Krausz, Nature Phys. **3**, 381 (2007).
[8] T. D. Donnelly *et al.*, Phys. Rev. Lett. **76**, 2472 (1996).
[9] J. W. G. Tisch *et al.*, J. Phys. B **30**, L709 (1997).
[10] C. Vozzi *et al.*, Appl. Phys. Lett. **86**, 111121 (2005).
[11] R. A. Ganeev *et al.*, J. Appl. Phys. **103**, 063102 (2008).
[12] M. Lein *et al.*, Phys. Rev. A **66**, 023805 (2002).
[13] R. de Nalda *et al.*, Phys. Rev. A **69**, 031804 (2004).
[14] T. Kanai, S. Minemoto, and H. Sakai, Nature (London) **435**, 470 (2005).
[15] M. Lein, J. Phys. B **40**, R135 (2007), and references therein.
[16] N. Hay *et al.*, Phys. Rev. A **61**, 053810 (2000).
[17] A. Ballard, K. Bonin, and J. Louderback, J. Chem. Phys. **113**, 5732 (2000).
[18] I. V. Hertel *et al.*, Phys. Rev. Lett. **68**, 784 (1992).
[19] S. W. J. Scully *et al.*, Phys. Rev. Lett. **94**, 065503 (2005).
[20] V. R. Bhardwaj, D. M. Rayner, and P. B. Corkum, Phys. Rev. Lett. **91**, 203004 (2003).
[21] V. R. Bhardwaj, D. M. Rayner, and P. B. Corkum, Phys. Rev. Lett. **93**, 043001 (2004).
[22] A. Jaroń-Becker, A. Becker, and F. H. M. Faisal, Phys. Rev. Lett. **96**, 143006 (2006).
[23] H. Hoshi *et al.*, Jpn. J. Appl. Phys. **36**, 6403 (1997).
[24] G. P. Banfi *et al.*, Phys. Rev. B **56**, R10 075 (1997).
[25] D. Bauer *et al.*, Phys. Rev. A **64**, 063203 (2001).
[26] H. Kafafi *et al.*, Chem. Phys. Lett. **188**, 492 (1992).
[27] M. F. Ciappina, A. Becker, and A. Jaroń-Becker, Phys. Rev. A **76**, 063406 (2007); **78**, 029902(E) (2008).
[28] G. P. Zhang, Phys. Rev. Lett. **95**, 047401 (2005).
[29] R. A. Ganeev *et al.*, Phys. Lett. A **339**, 103 (2005).
[30] L. B. Elouga Bom *et al.*, Phys. Rev. A **75**, 033804 (2007).
[31] J. Zanghellini, Ch. Jungreuthmayer, and T. Brabec, J. Phys. B **39**, 709 (2006).
[32] M. Ruggenthaler, S. V. Popruzhenko, and D. Bauer, Phys. Rev. A **78**, 033413 (2008).